Available online at www.sciencedirect.com
ScienceDirect
European Journal of Medicinal Chemistry 43 (2008) 189–203
EUROPEAN JOURNAL OF MEDICINAL CHEMISTRY
http://www.elsevier.com/locate/ejmech

Preliminary communication

Synthesis of *N*-(5,7-diamino-3-phenyl-quinoxalin-2-yl)-3,4,5-substituted anilines and *N*-[4[(5,7-diamino-3-phenylquinoxalin-2-yl)amino]benzoyl]-L-glutamic acid diethyl ester: Evaluation of in vitro anti-cancer and anti-folate activities

Paola Corona [a,*], Mario Loriga [a], M. Paola Costi [b], Stefania Ferrari [b], Giuseppe Paglietti [a]

[a] *Dipartimento Farmaco Chimico Tossicologico, Università degli Studi di Sassari, Via Muroni 23/A, 07100 Sassari, Italy*
[b] *Dipartimento di Scienze Farmaceutiche, Università degli Studi di Modena e Reggio Emilia, Via Campi 183, 41100 Modena, Italy*

Received 1 December 2006; received in revised form 17 March 2007; accepted 26 March 2007
Available online 18 April 2007

Abstract

Several diamino quinoxalines were designed, synthesized and evaluated as anti-tumor agents. Two compounds showed the most potent cytotoxic activities against the leukemia CCRF-CEM cell line ($GI_{50} < 0.01$ μM) and the ovarian cancer cell line OVCAR-4 ($GI_{50} = 0.03$ μM), respectively, with comparable/better activities than Methotrexate (MTX). Docking calculations of the complexes of hDHFR with the most active compounds identified the binding mode of the described molecules with respect to MTX.

Keywords: 5,7-Diaminoquinoxaline; Ovarian carcinoma; Leukemia; Anti-folate

1. Introduction

Despite continuous research efforts carried out on the discovery of safer or more potent anti-cancer compounds from a recent survey of these results [1] in the past decade only two new agents have been introduced as anti-cancer endowed with strong thymidilate synthase (TS) inhibitory activity (Tomudex and Pemetrexed). However, a few quinoxaline derivatives out of those described by us were reported as anti-cancer agents and among these a recent patent of 7-fluoro -4-hydrazinopyrrolo[1,2-*a*]quinoxalines as inhibitors of angiogenesis has appeared [2] providing a new way to stop cancer cell growth.

Contributions of our research group in this field have considered the design of structurally related pteridine compounds as novel anti-cancer agents. Thus, with the aim to discover a new class of classical and non-classical anti-folate agents, we replaced the pteridine and quinazoline nucleus present in the most active anti-cancer agents Metotrexate (MTX), Trimetrexate (TMQ) and Piritrexim (PTX) (Fig. 1) with the quinoxaline ring functionalised with a trifluoromethyl or amino group, or both, that bioisosterically could modulate the affinity for DHFR and TS enzymes. The wide range of compounds synthesized and evaluated as anti-tumor agents at the National Cancer Institute of Bethesda (NCI) allowed us to establish some structure–activity relationships, which can be summarized as follows: (i) bioisosterism of quinoxaline with the pteridine ring has shown to be profitable for the biological activity; (ii) compounds bearing a trifluoromethyl group at position 6 or 7 of the heterocycle and a phenyl group at position 3 resulted to be more active than the unsubstituted ones; (iii) the concomitant presence of both the trifluoromethyl group at position 6 and amine group at position 8, whatever be the substituent present at positions 2 and 3, increases the anti-cancer activity [3–17].

* Corresponding author. Tel.: +39079228764; fax: +39079228720.
E-mail address: pcorona@uniss.it (P. Corona).

0223-5234/$ - see front matter © 2007 Elsevier Masson SAS. All rights reserved.
doi:10.1016/j.ejmech.2007.03.035

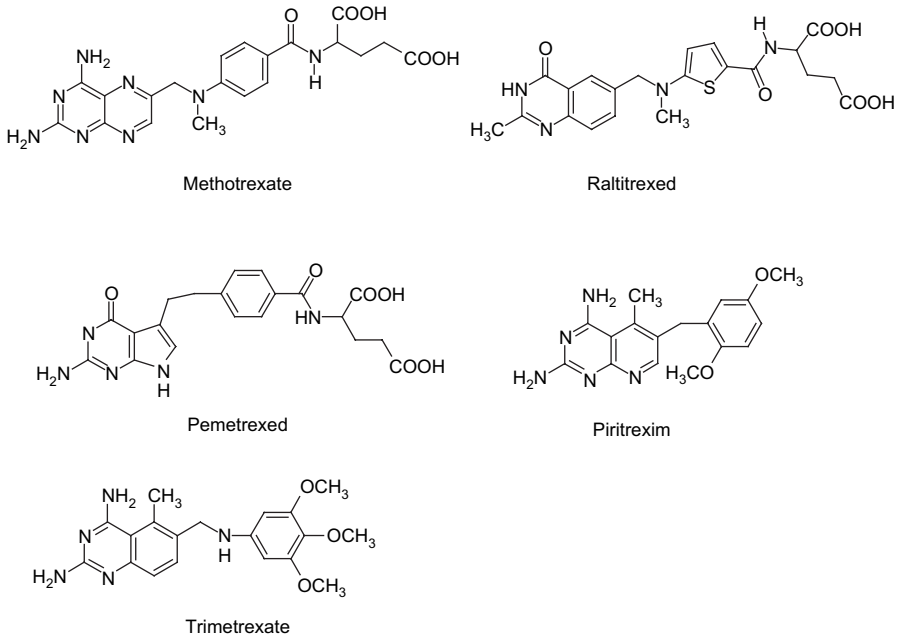

Fig. 1. Chemical structure of some classical and non-classical anti-folates.

In our previous work, we have described compounds **1a** and its analogues **1b–i** (Fig. 2) in which a phenyl ring was added at position 3 of the heterocycle as a lypophilic hindering group [3,5]. The screening performed at NCI has shown that many of the quinoxaline derivatives exhibited promising in vitro total growth inhibition and compound **1a** (NSC 637404) (Fig. 2) has been selected for in vivo screening [3]. Nevertheless, a certain number of the quinoxalines derivatives of classical and non-classical type have shown anti-folate activity against both murine and human DHFR [9,13].

Now, we extended our investigation taking into account that phenyl ring substitution at position 3 yielded the best result for in vitro anti-cancer activity and introduction of two amino groups at 5 and 7 positions of the quinoxaline ring might reproduce the most bioisosterical substitution with the pyrimidine ring of the classical anti-folates MTX, TMQ and PTX. At the same time, this replacement might also selectively improve their affinity towards the human DHFR (hDHFR) enzyme [18–22] and maintain the same binding mode as MTX in their X-ray crystal structure with hDHFR. With this in mind, in this paper we have designed compounds **2a–g** (Fig. 3) for an evaluation of their anti-cancer activity and comparison of their properties with those of the previously investigated quinoxalines **1a–i** [3,5]. In addition the enzyme inhibition activity against human TS (hTS) and DHFR was determined to evaluate their sub-cellular selectivity and potency. Along with the diamino compounds (**2a–g**), the 5,7-dinitro intermediates (**11–17**), were also tentatively subjected to enzymatic assay against three different species of TS such as, *Escherichia coli* TS (EcTS), *Lactobacillus casei* TS, and hTS and the results are presented here.

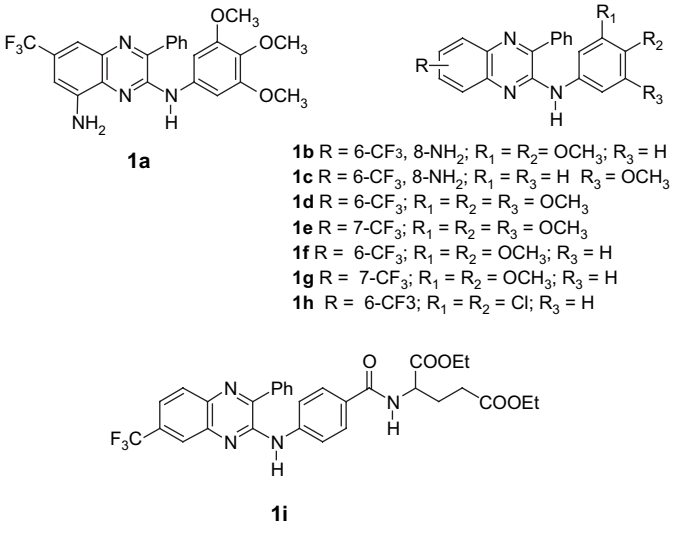

Fig. 2. First series of quinoxaline non-classical anti-folates [3,5].

At the end we have afforded a preliminary investigation of molecular modelling on compounds **2a–d**, which were selected, based on their inhibitory activity against hDHFR enzyme. Their binding mode to the target enzyme was studied using the molecular docking program Autodock 3.05 and the interesting results suggest further X-ray crystal structure studies with hDHFR.

2. Results and discussion

2.1. Chemistry

The preparation of the compounds **2a–g** was accomplished according to the reactions described in Scheme 1. 5,7-Dinitro-3-phenyl-2-chloroquinoxaline (**3**) underwent nucleophilic attack by the corresponding anilines **4–10** given in Scheme 1

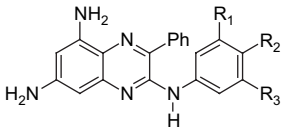

2a-f

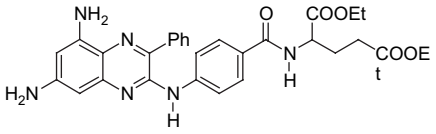

2g

Compd	R^1	R^2	R^3
2a	H	OCH_3	H
2b	OCH_3	H	OCH_3
2c	OCH_3	OCH_3	H
2d	OCH_3	OCH_3	OCH_3
2e	Cl	Cl	H
2f	H	F	H

Fig. 3. Designed compounds **2a–f** and **2g**.

in refluxing 1-propanol to give the 5,7-dinitro-3-phenyl-2-anilino substituted quinoxalines **11–17**. In the case of ester **17**, ethanol was alternatively used and heating at 80 °C was prolonged for 186 h. The desired 5,7-diamino-3-phenylquinoxalines **2a–g** were obtained by reduction with an excess of hydrazine hydrate in ethanol and in the presence of 10% palladised charcoal.

5,7-Dinitro-3-phenyl-2-chloroquinoxaline (**3**) is a new compound and has been prepared according to the reactions outlined in Scheme 2. Picric acid (**18**) was converted with $POCl_3$ in the presence of *N*,*N*-dimethylaniline into the 2-chloro-1,3,5-trinitrobenzene (**19**), which, once heated in a sealed vessel at 150 °C with a solution of ammonia saturated with propanol, yielded the 2,4,6-trinitroanilina (**20**). Selective reduction with H_2S and diluted ammonia gave the 2-amino-3,5-dinitrophenylamine (**21**) then cyclised regioselectively into the isomer 5,7-dinitro-quinoxalin-2(1*H*)one (**22**) (yield 80%) with benzoyl formic acid (**23**) under acidic catalysis [23–26]. A small amount (yield 2%) of the isomer 6,8-dinitro-quinoxalin-2(1*H*)one (**24**) was also obtained. This result was in good accordance with what some of us reported in a previous paper where it was demonstrated that when the two amino groups have different basicities, the ratio of the isomeric quinoxalinones is dependent on both the nature and *para*/*meta* position of the substituent. The more basic amino group undergoes protonation [26]. Unambiguous structure to the pairs of isomers **22** and **24** was assigned on the basis of NOE difference experiments carried out on isomer **22**. In fact, only in this case the proton at position 8 of 5,7-dinitro-3-phenyl quinoxaline-2(1*H*)one (**22**) experienced NOE interactions, greatly enhancing the resonance located at δ 8.25 by coupling with the amidic proton at position 1 (Fig. 4), whereas for isomer **24** no NOE interactions between aromatic protons and the amidic proton are possible and were not observed.

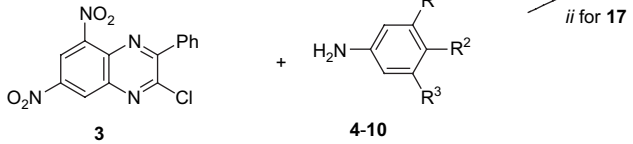

3

4-10

Anilines	R^1	R^2	R^3
4	H	OCH_3	H
5	OCH_3	H	OCH_3
6	OCH_3	OCH_3	H
7	OCH_3	OCH_3	OCH_3
8	Cl	Cl	H
9	H	F	H
10	H	CO-GlU-Et	H

i

ii for **17**

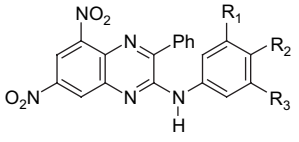

11-17

Compd	R^1	R^2	R^3
11	H	OCH_3	H
12	OCH_3	H	OCH_3
13	OCH_3	OCH_3	H
14	OCH_3	OCH_3	OCH_3
15	Cl	Cl	H
16	H	F	H
17	H	CO-GlU-Et	H

iii

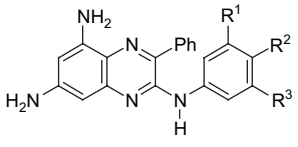

2a-g

Scheme 1. Synthesis of **2a–g**. Reagents and conditions: (i) 1-propanol, reflux for 1 h–72 h. (ii) EtOH, reflux for 186 h. (iii) NH_2–NH_2/H_2O, Pd/C, EtOH reflux for 10 min–2 h and 45 min.

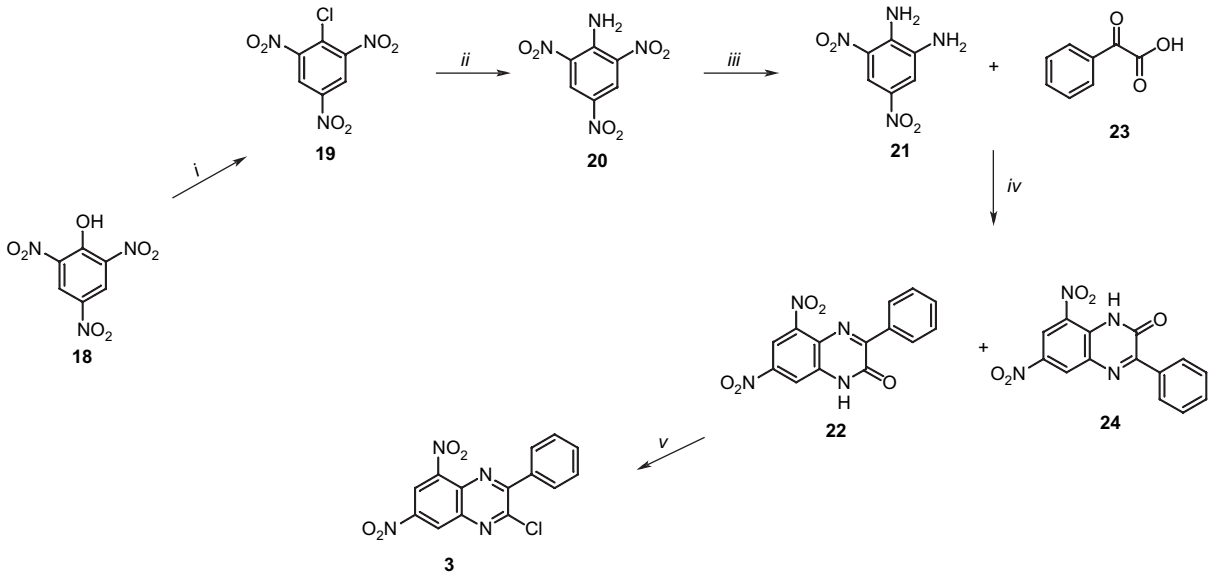

Scheme 2. Synthesis of **3**. Reagents and conditions: (i) $POCl_3$, *N*,*N*-dimethylaniline, room temperature for 15 min, (ii) 1-propanol saturated with gaseous NH_3, 100 °C for 3 h, (iii) EtOH, NH_4OH, H_2S, 45–50 °C, 30 min, (iv) EtOH, HCl 4 N, reflux for 1 h 50 min, (v) $POCl_3$, DMF anydrous, reflux for 2 h.

A further confirmation of this assignment came from the examination of ^{1}H NMR spectrum which showed downfield shift by 0.67 of the proton *peri* to the amidic group in isomer **22** [27–30]. Eventually the 5,7-dinitroquinoxalin-2(1*H*)one (**22**) was converted into the chloroquinoxaline (**3**) by treatment with $POCl_3$.

2.2. Anti-cancer activity

Evaluation of anti-cancer activity of the diamino quinoxalines synthesized (**2a–g**) was performed at the NCI. First, all diamino quinoxalines were evaluated in primary anti-cancer assay at 10^{-4} M concentration against NCI – H460 (lung), MCF7 (breast), and SF-268 (CNS) cell lines. For NCI criteria, compounds which reduce the growth of any one of the cell lines to approximately 32% or less are passed on for evaluation in the full panel of cell lines over a 5-log dose range. Quinoxalines **2a–g** which meet these criteria were evaluated for their anti-cancer activity following the known in vitro disease-oriented anti-tumor screening program which is based upon use of a multiple panels of 60 human tumor cell lines [31–33]. The anti-cancer activity of a tested compound is given by three parameters for each cell line: $\log_{10} GI_{50}$ value (GI_{50} = molar concentration of the compound that inhibits 50% net cell growth), $\log_{10} TGI$ value (TGI = molar concentration of the compound leading to total inhibition of net cell growth), and $\log_{10} LC_{50}$ value (LC_{50} = molar concentration of the compound leading to 50% net cell death). Furthermore, a mean graph midpoint (MG_MID) is calculated for each of the mentioned parameters, giving an averaged activity parameter over all cell lines. The anti-cancer activity of each compound is deduced from dose–response curves.

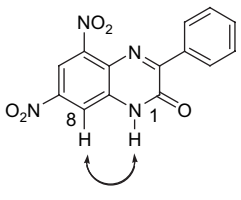

5,7-dinitro-quinoxalin-2(1H)one (**22**)

Fig. 4. NOE correlations for compound **22**.

The $\log_{10} GI_{50}$, $\log_{10} TGI$ and $\log_{10} LC_{50}$ values provided by NCI for compounds **2a–g** are reported in Tables 1 and 2. The data showed that all the compounds exhibited moderate activity against one or more human tumor cell lines. Compounds **2b** and **2d** have showed the most interesting values of cytotoxicity ($\log_{10} GI_{50}$) against leukemia CCRCEM and ovarian cancer OVCAR-4 cell lines, respectively. Moreover, different cancer cell lines of the same tumor type possessed a variable response to inhibition of growth in the presence of the new derivatives. For example, the OVCAR-4 ovarian cancer cells were susceptible to inhibition by **2d** ($\log_{10} GI_{50} = -7.50$, $\log_{10} TGI = -6.05$, $\log_{10} LC_{50} = -4.59$), whereas other ovarian cancer cell lines (such as IGROV1, OVCAR-3, OVCAR-5) showed a much lower level of inhibition ($\log_{10} GI_{50}$ ranged from −4.85 to −4.64). A similar situation has been highlighted in the case of diverse leukemia cell lines, with compound **2b** acting selectively as a potent inhibitor ($\log_{10} GI_{50} < -8.00$, $\log_{10} TGI = -6.78$, $\log_{10} LC_{50} = -6.01$) against the CCRF-CEM line, whereas other leukemia cell lines such as HL-60 (TB), K-562 and SR did not reach comparable TGI and LC_{50} levels. The RPMI-8226 cell line of this tumor type exhibited a lower level of inhibition ($\log_{10} GI_{50} = -5.90$, $\log_{10} TGI = -4.98$, $\log_{10} LC_{50} = -4.49$).

In Table 3, we showed the mean graph midpoint values of $\log_{10} GI_{50}$, log TGI_{50} and $\log_{10} LC_{50}$ for compounds **2a–g** in comparison with MTX. From these data, two compounds (**2b** and **2e**) emerged with an average $\log_{10} GI_{50} < -5.0$.

Table 1
Inhibition of in vitro cancer lines by selected 5,7-diamino-3-phenyl-2-anilino-quinoxalines, **2a–d**[a]

Panel cell line	Response parameters: (A) log GI_{50}[b] [M], (B) log TGI[c] [M], (C) log LC_{50}[d] [M]											
	Compound **2a**			Compound **2b**			Compound **2c**			Compound **2d**		
	A	B	C	A	B	C	A	B	C	A	B	C
Leukemia												
CCRF-CEM	−4.92	[e]	[e]	<−8.00	−6.78	−6.01	–	–	–	−5.36	−4.38	[e]
HL-60(TB)	−4.46	[e]	[e]	−5.00	[e]	[e]	–	–	–	−5.18	−4.63	−4.19
K-562	−4.53	[e]	[e]	−4.56	[e]	[e]	−4.69	−4.15	[e]	−4.90	−4.40	[e]
RPMI-8226	−4.72	[e]	[e]	−5.90	−4.98	−4.49	−5.10	−4.55	−4.06	−4.91	−4.49	−4.07
SR	−4.72	[e]	[e]	−5.25	[e]	[e]	−5.57	−4.66	[e]	−5.48	−4.80	−4.14
MOLT-4	–	–	–	–	–	–	−5.16	[e]	[e]	−5.59	−4.74	−4.25
Non-small cell lung cancer												
A549/ATCC	−4.56	[e]	[e]	−4.70	[e]	[e]	−4.45	[e]	[e]	−4.53	[e]	[e]
EKVX	−4.59	[e]	[e]	−4.88	−4.19	[e]	−4.59	−4.15	[e]	−4.75	−4.32	[e]
HOP-62	−4.56	[e]	[e]	−4.71	−4.27	[e]	−4.46	[e]	[e]	−4.79	−4.46	−4.14
HOP-92	−4.70	−4.28	[e]	–	–	[e]	–	–	–	−5.56	−4.68	−4.04
NCI-H226	−4.62	−4.01	[e]	−5.54	−4.48	[e]	−4.73	−4.24	[e]	–	–	–
NCI-H23	−4.90	−4.60	−4.29	−4.56	[e]	[e]	−4.58	−4.10	[e]	−4.60	−4.12	[e]
NCI-H322M	−4.63	−4.08	[e]	−4.86	−4.23	[e]	−4.60	[e]	[e]	−4.61	−4.10	[e]
NCI-H460	−4.57	−4.05	[e]	−5.10	−4.28	[e]	−4.69	[e]	[e]	−4.77	−4.28	[e]
NCI-H522	−4.83	−4.55	−4.28	−5.02	−4.54	−4.07	−4.54	[e]	[e]	−4.74	−4.27	[e]
Colon cancer												
COLO 205	−4.80	−4.53	−4.27	−4.84	−4.50	−4.17	−4.70	−4.39	−4.07	−4.85	−4.57	−4.28
HCC-2998	−4.55	[e]	[e]	−4.61	[e]	[e]	−4.74	−4.40	−4.07	–	–	–
HCT-116	−4.83	−4.55	−4.28	−4.77	−4.27	[e]	−4.83	−4.53	−4.23	−4.81	−4.47	−4.12
HCT-15	−4.82	−4.35	[e]	−4.70	[e]	[e]	−4.54	[e]	[e]	−4.82	−4.34	[e]
HT29	−4.62	−4.37	−4.05	−4.56	[e]	[e]	−4.60	−4.28	[e]	−4.48	−4.46	−4.13
KM12	−4.80	−4.51	−4.22	−4.88	−4.51	−4.14	−4.83	−4.49	−4.16	−4.97	−4.53	−4.09
SW-620	−4.65	4.43	−4.22	−4.57	[e]	[e]	−4.81	−4.44	−4.08	−4.62	[e]	[e]
CNS Cancer												
SF-268	−4.89	−4.51	−4.14	−5.25	−4.25	[e]	−4.85	−4.33	[e]	−4.74	−4.22	[e]
SF-295	−4.50	[e]	[e]	−4.90	−4.23	[e]	−4.77	−4.34	[e]	−4.80	−4.37	[e]
SF-539	–	–	–	–	–	–	−4.79	−4.43	−4.06	−4.83	−4.54	−4.25
SNB-19	−4.47	[e]	[e]	−4.24	[e]	[e]	−4.45	[e]	[e]	−4.48	[e]	[e]
SNB-75	−4.84	−4.37	[e]	−5.43	−4.35	[e]	–	–	–	–	–	–
U251	−4.79	−4.53	−4.26	−4.64	[e]	[e]	−4.59	[e]	[e]	−4.61	[e]	[e]
Melanoma												
LOX IMVI	−4.79	−4.53	−4.26	−4.82	−4.30	[e]	−4.59	−4.14	[e]	−4.73	−4.31	[e]
MALME-3M	−4.82	−4.55	−4.27	−5.36	−4.61	[e]	−4.80	−4.45	−4.09	−4.89	−4.55	−4.21
M14	−4.75	−4.44	−4.12	−4.85	−4.46	−4.07	−4.68	−4.16	[e]	−4.71	−4.35	[e]
SK-MEL-2	−4.81	−4.50	−4.20	−4.92	−4.20	[e]	−4.57	[e]	[e]	−4.80	−4.45	−4.11
SK-MEL-28	−4.77	−4.52	−4.26	−4.83	−4.05	[e]	−4.67	−4.30	[e]	−5.84	−4.68	−4.20
SK-MEL-5	−4.82	−4.54	−4.27	−4.98	−4.52	−4.06	−4.91	−4.59	−4.27	−4.89	−4.56	−4.23
UACC-257	−4.84	−4.56	−4.28	−4.80	−4.32	[e]	−4.45	[e]	[e]	−4.53	[e]	[e]
UACC-62	−4.77	−4.52	−4.26	−5.13	−4.63	−4.21	−4.87	−4.56	−4.25	−4.87	−4.50	−4.13
Ovarian cancer												
IGROV1	−4.81	−4.45	−4.08	−5.57	−4.77	[e]	−4.61	[e]	[e]	−4.80	−4.24	[e]
OVCAR-3	−4.76	−4.43	−4.10	−5.41	−4.70	−4.00	−4.52	[e]	[e]	−4.85	−4.43	−4.01
OVCAR-4	−4.98	−4.66	−4.33	−4.75	[e]	[e]	−4.73	−4.28	[e]	−7.50	−6.05	−4.59
OVCAR-5	−4.67	−4.27	[e]	−4.58	[e]	[e]	−4.53	−4.14	[e]	−4.67	−4.33	[e]
OVCAR-8	−4.86	−4.51	−4.17	−5.21	−4.33	[e]	−4.47	[e]	[e]	−4.81	−4.46	−4.10
SK-OV-3	−4.48	−4.01	[e]	−5.18	−4.40	[e]	−4.42	−4.06	[e]	−4.64	−4.24	[e]
Renal cancer												
786-0	−4.80	−4.51	−4.22	−4.75	−4.29	[e]	−4.62	−4.04	[e]	−4.84	−4.39	[e]
A498		[e]	[e]	−5.31	−4.65	−4.10	−4.93	−4.25	[e]	−4.50	[e]	[e]
ACHN	−4.82	−4.36	[e]	−5.25	−4.08	[e]	−4.56	[e]	[e]	−4.78	−4.37	[e]
CAKI-1	−4.45	[e]	[e]	−4.83	−4.14	[e]	−4.74	−4.18	[e]	−4.81	−4.31	[e]
RXF 393	−4.96	−4.62	−4.27	−5.50	−4.73	−4.02	−5.09	−4.31	[e]	−4.84	−4.46	−4.08
SN12C	−4.69	−4.24	[e]	−5.06	[e]	[e]	−4.78	−4.36	[e]	−4.69	−4.08	[e]
TK-10	−4.78	−4.37	[e]	−4.88	−4.37	[e]	−4.68	−4.23	[e]	−4.62	−4.18	[e]
UO-31	−4.78	−4.47	−4.15	−5.05	−4.35	[e]	−4.55	[e]	[e]	−4.82	−4.04	[e]
Prostate cancer												
PC-3	−4.68	−4.32	[e]	−5.71	−4.96	−4.24	−4.85	−4.44	−4.03	−4.85	−4.23	[e]
DU-145	−4.41	[e]	[e]	−4.64	[e]	[e]	−4.35	[e]	[e]	−4.66	−4.13	[e]

(*continued on next page*)

Table 1 (*continued*)

Panel cell line	Response parameters: (A) log GI_{50}[b] [M], (B) log TGI[c] [M], (C) log LC_{50}[d] [M]											
	Compound **2a**			Compound **2b**			Compound **2c**			Compound **2d**		
	A	B	C	A	B	C	A	B	C	A	B	C
Breast cancer												
MCF7	−4.83	−4.55	−4.28	−5.10	−4.57	−4.07	−4.69	−4.35	−4.01	−4.59	−4.02	[e]
NCI/ADR-RES	−4.72	−4.35	[e]	−4.89	−4.13	[e]	−4.76	−4.37	[e]	−4.84	−4.36	[e]
MDA-MB-231/ATCC	−4.94	−4.60	−4.26	−5.19	−4.46	[e]	−5.31	−4.73	−4.33	−4.95	−4.53	−4.11
HS 578T	−4.84	−4.33	[e]	−4.96	−4.20	[e]	−4.73	−4.30	[e]	−4.82	−4.11	[e]
MDA-MB-435	−4.78	−4.52	−4.26	−4.94	−4.62	−4.31	−4.79	−4.49	−4.20	−5.13	−4.61	−4.16
MDA-N	−4.67	−4.44	−4.22	−4.89	−4.44	−4.00	–	–	–	−4.98	−4.50	−4.03
BT-549	−4.87	−4.50	−4.12	−5.33	−4.50	[e]	−4.59	−4.09	[e]	−4.77	−4.47	−4.17
T-47D	−4.75	−4.27	[e]	−5.35	−4.64	[e]	−4.84	−4.42	[e]	−5.22	−4.56	−4.02

–Cell line not tested.

[a] Data obtained from the NCI's in vitro disease-oriented human tumor cells screen (see Refs. [19–21]).

[b] The log of the molar concentration that inhibits 50% net cell growth.

[c] The log of the molar concentration giving total growth inhibition.

[d] The log of the molar concentration leading to 50% net cell death.

[e] The values of log GI_{50}, log TGI or log LC_{50} >-4.00.

In Table 4, we represented the average of $\log_{10} GI_{50}$ for each cancer type to put in evidence both activity and selectivity. All but compound **2a** showed particular selectivity against leukemia cell lines. Best results were obtained with compounds **2b** and **2e** against leukemia cell lines ($\log_{10} GI_{50} = 5.74$ and 5.60, respectively) whereas compound **2e** recorded a MG_MID $\log_{10} GI_{50} = -5.08$, which accounts for the highest micromolar activity against all cell lines.

In Table 5, we compared the activities of the most active compounds **2b** and **2d**, on leukemia (CCRF-CEM) and ovarian (OVCAR-4) cell lines, respectively, with that recorded for MTX. Compound **2b** showed an anti-cancer activity against leukemia (CCRF-CEM) better than that recorded for MTX which is taken from Ref. [34].

The results thus obtained allowed some considerations about structure and in vitro tumor inhibitory activity relationships. It is evident that all but compound **2a** are, on average, very active against leukemia cell lines. When two methoxy groups are present in the side chain, the best activity was recorded for the 3′,4′-disubstituted compound (**2b**), while in the case of three methoxy groups (**2d**) the increase of lipophilicity produce an unfavourable effect on $\log_{10} GI_{50}$. Replacement of the two methoxy groups in the anilino moiety (**2b**) with chlorine (**2e**) seems to increase the anti-cancer activity on the whole. Fluorine in 4′ position slightly increases the activity only on comparison with that of **2a** and **2c**.

When we compare the $\log_{10} GI_{50}$ of this series with that of the corresponding previously described compounds that bear the trifluoromethyl group in quinoxaline benzene counterpart (Table 6), it is worth noting that in all cases the increase of potency is due to the presence of the two amino groups [3,5].

2.3. Anti-folate activity

In Table 7, the enzyme inhibition activity profiles for compounds **2a–g**, **11–15**, **17** towards hDHFR and a panel of three TS enzymes are reported.

Compounds **2a**, **2b** and **2d** are active against hDHFR with Ki in the range 0.1–1.8 μM. The best compound is **2d**. Compounds **2b** and **2d** are selective towards hDHFR with respect to hTS with selectivity indices (Ki hTS/Ki hDHFR) of 42 and 510, respectively. Compounds **2c**, **2e–g** are not active at 10 μM. Compound **2e** is the best inhibitor towards hTS with Ki of 0.9 μM, while **2a**, **2b**, **2d** and **2g** are moderate hTS inhibitors showing Ki ranging between 6 and 51 μM. Compounds **2e** and **2g** are selective towards hTS with respect to hDHFR. Compounds **2c** and **2f** are not active at 10 μM.

From these data it appears that the methoxy groups contribute to the increasing affinity towards hDHFR (**2a**, **2b**, **2d**) with respect to hTS. The substituition of the methoxy group with the chlorine (**2e**) or fluorine (**2f**) increases the affinity for hTS (**2e**), but loses it's affinity for hDHFR.

Interestingly, among the 5,7-dinitro intermediates (**11–17**), which were considered as precursors of the diamino derivatives, compound **11** was by far the best inhibitor showing quite the same Ki as **2e** (Ki hTS = 0.7 μM). Other compounds are also active with Ki in the range of 2.1–36 μM.

Dinitro intermediates (**11–15**, **17**) are more active with respect to the corresponding diamino compounds (**2a–e**, **2g**) except for **2e** and **15**. However, along these two series the same trend is not observed. While the dichloro derivative (**2e**) is the most active compound in the diamino series (Ki hTS = 0.9 μM), the dichloro dinitro intermediate (**15**) is the worst compound of the dinitro series (Ki hTS = 36 μM). Analogously while the dimethoxy derivatives in the dinitro series (**12**, **13**) show the same activity towards hTS (Ki hTS = 14–15), the two dimethoxy derivatives in the diamino series (**2b**, **2c**) show very different Ki towards hTS (Ki hTS = 25 and no inhibition at 10 μM).

In regard to the activity towards bacterial TS, compound **15** is the best with a Ki of 0.2 μM towards EcTS and being species-specific with respect to hTS with a specificity index (Ki hTS/Ki EcTS) of 180. Also, compounds **2e**, **13** and **17** show good activity towards EcTS (Ki EcTS = 1–3 μM), but they are not species-specific inhibiting hTS (Ki hTS = 0.9–16).

Table 2
Inhibition of in vitro cancer lines by selected 5,7-diamino-3-phenyl-2-anilino-quinoxalines **2e–g**[a]

Panel cell line	Response parameters: (A) log GI_{50}[b] [M], (B) log TGI[c] [M], (C) log LC_{50}[d] [M]								
	Compound **2e**			Compound **2f**			Compound **2g**		
	A	B	C	A	B	C	A	B	C
Leukemia									
CCRF-CEM	−5.89	–	[e]	–	–	–	−5.53	[e]	[e]
HL-60(TB)	−5.59	−4.14	[e]	−4.95	[e]	[e]	−5.02	−4.29	[e]
K-562	−5.45	[e]	[e]	−5.30	[e]	[e]	–	–	–
MOLT-4	−5.39	[e]	[e]	[e]	[e]	[e]	−5.62	−5.13	[e]
RPMI-8226	−5.70	−5.31	[e]	−5.33	−4.46	[e]	−5.50	[e]	[e]
SR	−5.59	−4.81	[e]	−5.27	–	–	–	–	–
Non-small cell lung cancer									
A549/ATCC	−4.97	−4.46	[e]	−4.76	−4.35	[e]	−4.70	[e]	[e]
EKVX	−5.42	−4.79	−4.32	−4.92	−4.52	−4.12	−4.54	[e]	[e]
HOP-62	−4.76	−4.42	−4.07	−4.42	[e]	[e]	−4.71	−4.40	−4.09
HOP-92	–	–	–	−4.88	−4.36	[e]	−4.97	−4.53	−4.09
NCI-H226	−4.76	−4.42	−4.09	−4.75	−4.32	[e]	−4.57	−4.26	[e]
NCI-H23	−4.72	−4.26	[e]	−4.65	−4.31	[e]	−4.73	−4.26	[e]
NCI-H322M	−4.84	−4.52	−4.20	−4.77	−4.45	−4.13	−4.38	[e]	[e]
NCI-H460	−5.80	−4.64	−4.25	−4.58	[e]	[e]	−5.07	−4.32	[e]
NCI-H522	−5.28	−4.66	−4.16	[e]	[e]	[e]	−4.56	[e]	[e]
Colon cancer									
COLO 205	−4.93	−4.50	−4.07	−4.69	−4.25	[e]	−5.05	[e]	[e]
HCC-2998	–	–	–	–	–	–	–	–	–
HCT-116	−4.97	−4.28	[e]	−4.70	[e]	[e]	−4.82	−4.29	[e]
HCT-15	−4.67	[e]	[e]	−4.90	−4.42	[e]	−4.63	[e]	[e]
HT29	–	–	–	−4.73	−4.45	−4.17	–	–	–
KM12	−5.23	−4.61	−4.06	−4.92	−4.53	−4.14	−4.55	[e]	[e]
SW-620	−4.88	−4.29	[e]	−4.87	−4.41	[e]	−4.39	[e]	[e]
CNS cancer									
SF-268	−4.92	−4.54	−4.17	−4.88	−4.39	[e]	−4.63	[e]	[e]
SF-295	−4.91	−4.55	−4.20	−4.84	−4.49	−4.14	−4.75	−4.36	[e]
SF-539	−4.77	−4.45	−4.14	−4.96	−4.61	−4.26	−4.56	[e]	[e]
SNB-19	−4.89	−4.52	−4.15	−4.66	−4.40	−4.14	−4.67	[e]	[e]
SNB-75	–	–	–	−4.68	−4.38	−4.07	–	–	–
U251	−5.33	[e]	[e]	−5.25	−4.70	−4.30	−4.70	−4.36	−4.02
Melanoma									
LOX IMVI	−5.36	[e]	[e]	−5.32	−4.74	−4.31	−5.07	[e]	[e]
MALME-3M	−4.99	−4.61	−4.24	–	–	–	−5.55	−5.21	[e]
M14	−4.83	−4.22	[e]	−4.79	−4.36	[e]	−5.60	−5.23	−4.12
SK-MEL-2	−5.63	−4.72	−4.16	−4.53	[e]	[e]	−5.11	−4.13	[e]
SK-MEL-28	−4.79	−4.35	[e]	−4.69	−4.41	−4.12	−5.82	−5.52	−5.23
SK-MEL-5	−4.96	−4.59	−4.23	−4.84	−4.48	−4.12	−5.18	−4.50	[e]
UACC-257	−4.94	−4.55	−4.16	−4.82	−4.54	−4.26	−5.70	−5.31	[e]
UACC-62	−4.88	−4.52	−4.17	−4.79	−4.50	−4.20	−5.45	−4.84	−4.19
Ovarian cancer									
IGROV1	−5.31	−4.68	−4.18	−4.78	[e]	[e]	−5.20	−4.05	[e]
OVCAR-3	−5.53	−5.00	−4.43	−5.33	−4.75	−4.29	−5.07	−4.50	[e]
OVCAR-4	−4.95	−4.32	[e]	−4.87	−4.31	[e]	−4.57	[e]	[e]
OVCAR-5	−4.55	−4.31	−4.07	−4.42	[e]	[e]	−4.46	−4.06	[e]
OVCAR-8	−5.29	−4.10	[e]	−4.91	−4.52	−4.13	−4.47	[e]	[e]
SK-OV-3	−4.86	−4.50	−4.15	−4.39	[e]	[e]	−4.66	−4.32	[e]
Renal cancer									
786-0	−4.83	−4.43	−4.03	−4.76	−4.27	[e]	−4.75	−4.43	−4.11
A498	−4.92	−4.58	−4.24	−4.76	−4.7	−4.18	–	–	–
ACHN	–	–	–	−4.99	−4.65	−4.31	−4.89	−4.33	[e]
CAKI-1	−4.87	−4.53	−4.19	−4.72	−4.39	−4.07	−4.56	[e]	[e]
RXF 393	−5.21	−4.51	[e]	−5.06	−4.54	−4.07	−4.61	−4.07	–
SN12C	−4.90	−4.50	−4.10	−4.80	−4.47	−4.13	–	–	–
TK-10	−4.86	−4.52	−4.18	−4.76	−4.45	−4.13	−4.48	−4.12	[e]
UO-31	−4.95	−4.44	[e]	−4.77	−4.21	[e]	−4.66	−4.12	[e]
Prostate cancer									
PC-3	−5.51	−4.82	−4.05	−4.93	[e]	[e]	−4.67	−4.04	[e]
DU-145	−4.78	−4.49	−4.20	−4.92	−4.55	−4.18	−4.35	[e]	[e]

(*continued on next page*)

Table 2 (*continued*)

Panel cell line	Response parameters: (A) log GI_{50}[b] [M], (B) log TGI[c] [M], (C) log LC_{50}[d] [M]								
	Compound **2e**			Compound **2f**			Compound **2g**		
	A	B	C	A	B	C	A	B	C
Breast cancer									
MCF7	−5.30	−4.68	−4.12	−4.90	[e]	[e]	−4.53	[e]	[e]
NCI/ADR-RES	−4.81	−4.26	[e]	−4.62	−4.24	[e]	−4.71	−4.20	[e]
MDA-MB-231/ATCC	−5.24	−4.56	[e]	−4.96	−4.52	−4.07	−5.05	−4.55	−4.09
HS 578T	−4.72	−4.29	[e]	−4.72	−4.23	[e]	−4.47	−4.12	[e]
MDA-MB-435	−5.67	−5.34	−5.01	−5.13	−4.68	−4.30	−4.92	−4.44	[e]
MDA-N	–	–	–	–	–	–	–	–	–
BT-549	–	–	–	−4.92	−4.57	−4.20	−4.38	[e]	[e]
T-47D	−4.94	−4.51	−4.08	–	–	–	−5.78	−5.31	[e]

– Cell line not tested.

[a] Data obtained from the NCI's in vitro disease-oriented human tumor cells screen (see Refs. [19–21]).

[b] The log of the molar concentration that inhibits 50% net cell growth.

[c] The log of the molar concentration giving total growth inhibition.

[d] The log of the molar concentration leading to 50% net cell death.

[e] The values of log GI_{50}, log TGI or log LC_{50} >-4.00.

Compounds **2c**, **2g**, **11**, **12**, **14** are not active towards EcTS at 10 μM. All compounds are moderately active towards LcTS with Ki in the range of 1–36 μM. Compounds **2c** and **2f** are species-specific with respect to hTS with specificity indices (Ki hTS/Ki LcTS) of 32 and 63, respectively.

2.4. Molecular docking

With the aim to describe the binding mode of compounds **2a–d** to their predicted intracellular target, the enzyme hDHFR, we attempted to rigidly superimpose compounds **2a–d** on the X-ray ternary complex hDHFR–NADPH–MTX [18–22]. The rigid matching failed due to geometry differences between the quinoxaline/pteridine derivatives. No X-ray structure of the 2,3-disubstitued quinoxaline derivatives complexed with DHFR enzymes is available yet. Therefore we suspected that the binding mode of the latter molecules could be different with respect to the classical binding mode adopted by the known pteridine derivatives, unless the enzyme does not accommodate the molecules with a large conformational change. This would be due to mainly the bulkiness of the phenyl in position 2 and the methoxyphenyl fragment at position 3. Classical folate analogues MTX (1U72, 1DLS) and their derivatives (1OHJ, 1OHK), pyrido[2,3-*d*]pyrimidine derivatives (1DLR, 1KMV, 1KMS, 1PD8), furo[2,3-*d*]pyrimidine derivatives (1HFQ, 1HFR, 1HFP), quinazoline derivatives (1S3W)) bind to hDHFR forming a stacking interaction with the nicotinamide ring of NADPH and also interact with Thr7, Val8, Ala9, Leu22, Glu30, Phe31 and Phe34, whereas the remaining part of the ligands are stretched along the active site hole interacting with Phe31, Phe34, Gln35, Ile60, Pro61, Asn64, Leu67 and Arg70.

Table 3
Log_{10} GI_{50}, log_{10} TGI, log_{10} LC_{50} mean graph midpoints (MG_MD) of in vitro cytotoxicity of compounds **2a–g** against human tumor cell lines. In square brackets the corresponding GI_{50}, TGI and LC_{50} values are expressed in μM

Compound	log GI_{50} [μM]	log TGI [μM]	log LC_{50} [μM]
2a	−4.73 [18.6]	−4.32 [47.9]	−4.11 [77.6]
2b	−5.04 [9.12]	−4.36 [43.6]	−4.07 [85.1]
2c	−4.72 [19.0]	−4.23 [58.9]	−4.03 [93.3]
2d	−4.90 [12.6]	−4.38 [41.7]	−4.07 [85.1]
2e	−5.08 [8.32]	−4.48 [33.1]	−4.11 [77.6]
2f	−4.82 [15.1]	−4.34 [45.7]	−4.08 [83.2]
2g	−4.87 [13.5]	−4.30 [50.1]	−4.04 [91.2]
MTX[a]	−6.33 [0.465]	−3.77 [171]	−3.61 [247]

[a] Values from NCI data base [34].

The complexes of compounds **2a–d** with hDHFR have been predicted using AutoDock 3.05. AutoDock results clearly show a preferred binding conformation for compounds **2a–d** that correspond to the conformation of the best clusters (lowest docked energy and most populated). AutoDock finds 31, 23, 55 and 60 clusters of binding conformations out of 100 runs for compounds **2a**, **2b**, **2c** and **2d**, respectively. The best binding conformation groups together 37, 39, 14 and 19 out of 100 runs for compounds **2a**, **2b**, **2c** and **2d**, respectively, with docked energies that range from −10.59 to −10.86 kcal/mol. Compounds **2a–d** bind in the same binding site and variation in number and position of the substituents on the phenyl ring does not alter their binding mode.

They bind in the active site of the enzyme in the area where the PABA-Glu fragment of MTX also binds with the pyrazine ring matching the benzene ring of the PABA fragment. The diamino quinoxaline ring is located perpendicular to the nicotin ring and to part of the nicotin ribose of the NADPH and also interacts with Phe31, Phe34, Thr56, Ser59 and Ile60, whereas the two phenyls in positions 2 and 3 are oriented towards the entrance of the active site and they interact with Phe31, Phe34, Gln35, Ile60, Pro61, Asn64, Leu67 and Arg70. (Fig. 5).

The amine in position 7 forms two hydrogen bonds with the side chain of Ser59 and the hydroxyl in position 2 of the ribose ring bound to the nicotine part of the cofactor. The methoxy groups in *para* and *meta* positions can hydrogen bind to Arg28 and Asn64. These ligands form ring–ring interactions

Table 4
Log_{10} GI_{50} mean graph midpoint (MG-MID) recorded in each cancer type[a] for compounds **2a–g**

Panel cell line	2a	2b	2c	2d	2e	2f	2g
Leukemia	−4.67	−5.74	−5.13	−5.24	−5.60	−5.21	−5.42
Non-small cell lung cancer	−4.66	−4.92	−4.58	−4.79	−5.07	−4.72	−4.69
Colon cancer	−4.72	−4.70	−4.72	−4.76	−4.94	−4.80	−4.69
CNS cancer	−4.70	−4.89	−4.69	−4.69	−4.96	−4.88	−4.66
Melanoma	−4.80	−4.96	−4.69	−4.91	−5.05	−4.82	−5.43
Ovarian cancer	−4.76	−5.12	−4.55	−5.21	−5.08	−4.78	−4.74
Renal cancer	−4.75	−5.08	−4.76	−4.74	−4.93	−4.83	−4.66
Prostate cancer	−4.54	−5.17	−4.60	−4.75	−5.14	−4.92	−4.51
Breast Cancer	−4.80	−5.08	−4.81	−4.91	−5.11	−4.87	−4.83
MG-MID	−4.73	−5.04	−4.72	−4.90	−5.08	−4.82	−4.87

[a] Each cancer type represents the average of six to eight different cancer cell lines.

with Phe31, Phe34 and the nicotine ring of NADPH. Moreover, they interact with Leu22, Pro26, Gln35, Thr56, Ile60, Pro61, Leu67, Arg70 and Val115 through van der Waals interactions (Fig. 6).

3. Conclusion

Compounds **2a**, **2c–e** and **2g** exhibited better anti-cancer activity with respect to the corresponding trifluoromethyl analogues (**1a–i**) (Table 6) [3,5]. Structure–activity relationships allow us to conclude that the presence of two amino groups on the quinoxaline system increases the anti-proliferative activity. Furthermore, compounds **2b** and **2d**, were the most potent of all derivatives tested, and displayed a high degree of selectivity against leukemia CCRF-CEM ($\log_{10} GI_{50} = <-8.00$, $\log_{10} TGI = -6.78$, $\log_{10} LC_{50} = -6.01$) and OVCAR-4 ($\log_{10} GI_{50} = -7.50, \log_{10} TGI = -6.05, \log_{10} LC_{50} = -4.59$), respectively (Table 1), and resulted even more active than MTX in these cell lines (Table 5). The same compounds have shown the most significant inhibitory activity against hDHFR: $Ki = 0.6$ μM for compound **2b** and $Ki = 0.1$ μM for compound **2d**. The calculated complex between hDHFR and compounds **2a–d** suggested that the binding mode of these quinoxaline derivatives are different with respect to that of MTX and this fact also accounts for a better activity recorded for the intermediate dinitro-derivatives in the enzyme assay. At this stage it is to be observed that a relationship between the enzyme inhibitory activity and anti-cancer activity for these compounds could not be traced owing to incontrovertible selection of our compounds affected at NCI.

These results are encouraging since inhibition of the folate enzymes seems to confirm the grounds for our original assumption. However, further studies are in progress to verify the effect of various substituents in position 2 and 3 of the 5, 7-diamino quinoxaline on the anti-tumor and anti-folate activities, and to avenue structural biology studies that could provide more detailed information for structure-based development of new molecules.

Table 5
Comparison of cytotoxicity evaluations ($\log_{10} GI_{50}$) for compounds **2b** and **2d** against selected tumor cell lines with MTX. In square brackets the corresponding GI_{50} values are expressed in μM

Compound	Cell line	$\log_{10} GI_{50}$ [μM]
2b	Leukemia CCRF-CEM	−8 [<0.01]
2d	Ovarian cancer OVCAR-4	−7.5 [0.0316]
MTX[a]	Leukemia CCRF-CEM	−7.4 [0.0398]
MTX[a]	Ovarian cancer OVCAR-4	−8.6 [0.00251]

[a] Values from NCI [34].

4. Experimental

4.1. Chemistry

4.1.1. General remarks

Melting points were carried out with a Köfler hot stage or Digital Electrothermal melting point apparatus and are uncorrected. Infrared spectra were recorded as nujol mulls on NaCl plates with a Perkin-Elmer 781 IR spectrophotometer and are expressed in ν (cm^{-1}). UV spectra are qualitative and were recorded in nm for solutions in EtOH with a Perkin-Elmer Lamba 5 spectrophotometer. Nuclear magnetic resonance (^1H NMR and NOE difference) spectra were determined in $CDCl_3$, DMSO-d_6, $CDCl_3$/DMSO-d_6 (in the ratio 1:3) and were recorded in a Varian XL-200 (200 MHz). Chemical shifts (δ scale) are reported in parts per million (ppm) downfield

Table 6
Anti-tumor activity ($\log_{10} GI_{50}$, $\log_{10} TGI$, $\log_{10} LC_{50}$, mean graph midpoints (MG-MID)) comparison between compounds **2a**, **2c–e**, **2g** and the corresponding trifluoromethyl analogues (**1a–i**) [3,5]. In square brackets the corresponding GI_{50} values are expressed in μM

Compound	$\log_{10} GI_{50}$ [μM]	$\log_{10} TGI$ [μM]	$\log_{10} LC_{50}$ [μM]
2a	−4.73 [18.6]	−4.32 [47.9]	−4.11 [77.6]
1c	−4.15 [70.8]	−4.00 [100]	−4.00 [100]
2c	−4.72 [19.0]	−4.23 [58.9]	−4.03 [93.3]
1b	−4.62 [24.0]	−4.20 [63.1]	−4.02 [95.5]
1f	−4.47 [33.9]	−4.08 [83.2]	−4.03 [93.3]
1g	−4.66 [21.9]	−4.18 [66.1]	−4.00 [100]
2e	−5.08 [8.32]	−4.48 [33.1]	−4.11 [77.6]
1h	−4.50 [31.6]	−4.00 [100]	−4.00 [100]
2d	−4.90 [12.6]	−4.38 [41.7]	−4.07 [85.1]
1a	−4.42 [38.0]	−4.08 [83.2]	−4.00 [100]
1d	−4.83 [14.8]	−4.23 [58.9]	−4.06 [87.1]
1e	−4.31 [49.0]	−4.11 [77.6]	−4.02 [95.5]
2g	−4.87 [13.5]	−4.30 [50.1]	−4.04 [91.2]
1i	−4.50 [31.6]	−4.00 [100]	−4.00 [100]

Table 7
Inhibition constant (Ki) for compounds **2a–g** and 5,7-dinitro intermediates (**11–17**)

Compound	LcTS Ki (μM)	EcTS Ki (μM)	hTS Ki (μM)	hDHFR Ki (μM)
2a	–	–	6	1.8
2b	–	–	25	0.6
2c	6	NI[a]	NI[a]	NI[a]
2d	–	–	51	0.1
2e	1	3	0.9	NI[a]
2f	3	70	NI[a]	NI[a]
2g	27	NI[a]	34	NI[a]
11	8	NI[a]	0.7	–
12	6	NI[a]	15	–
13	24	1	14	–
14	11	NI[a]	2.1	–
15	5	0.2	36	–
16	–	–	–	–
17	36	3	16	
MTX				4.42×10^{-6}[b]

[a] No inhibition at 10 μM.
[b] see Ref. [48].

from tetramethylsilane (TMS) as internal standar. Splitting patterns are designated, as follows: s, singlet; d, doublet; t, triplet; q, quadruplet; m, multiplet; br s, broad singlet; dd, double doublet.

The assignment of exchangeable protons (OH and NH) was confirmed by the addition of D_2O. MS spectra were performed on combined HP 5790-HP 5970 GC/MS apparatus or with a combined Liquid Chromatograph-Agilent 1100 series Mass Selective Detector (MSD). Analytical thin-layer chromatography (TLC) was performed on Merck silica gel F-254. Pure compounds showed a single spot in TLC. For flash chromatography, Merck silica gel 60 was used with a particle size

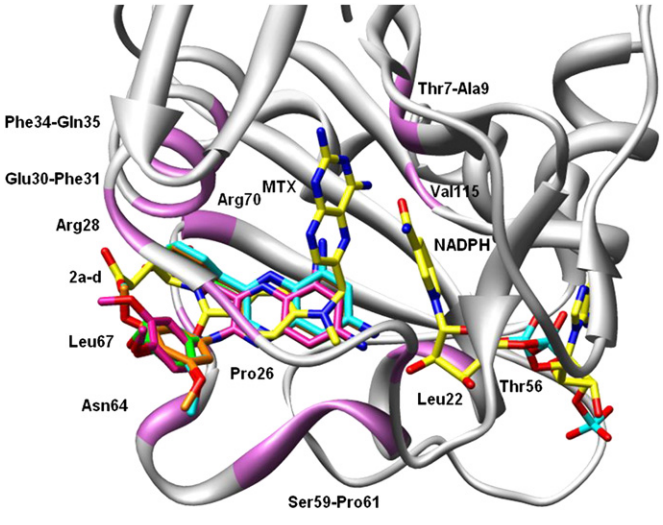

Fig. 5. Predicted binding modes for compounds **2a–d** (coloured by atom with carbon atoms in green, pink, orange and cyan, respectively, for compounds **2a**, **2b**, **2c** and **2d**) in the active site of hDHFR (only the ribbon representation of the protein, coloured in gray, is shown. The ribbon of key residues is coloured in violet.). Coloured by atom with carbon atoms in yellow are the NADPH cofactor and MTX (for interpretation of the references to colour in this figure legend, the reader is referred to the web version of this article).

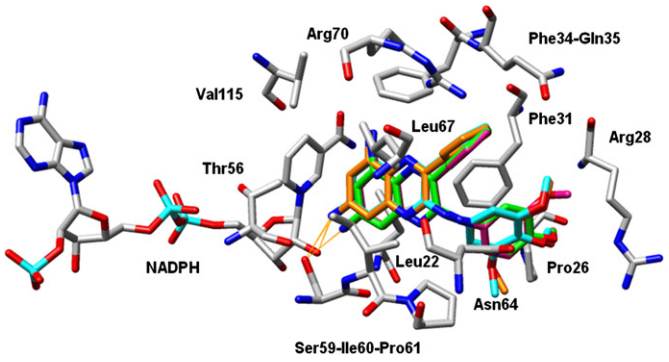

Fig. 6. Predicted binding modes for compounds **2a–d** (coloured by atom with carbon atoms in green, pink, orange and cyan, respectively, for compounds **2a**, **2b**, **2c** and **2d**) in the active site of hDHFR (only the interacting residues of the protein, coloured by atom with carbon atoms in gray, are shown. For interpretation of the references to colour in this figure legend, the reader is referred to the web version of this article).

0.040–0.063 mm (230–400 mesh ASTM). Elemental analyses were performed on a Perkin-Elmer 2400 instrument at Laboratorio di Microanalisi, Dipartimento di Chimica, Università di Sassari, Italy, and results were within ±0.4% of theoretical values.

4.1.2. Intermediates

2-Chloro-1,3,5-trinitrobenzene [23] (**19**) was prepared as reported in the literature [23]; 2,4,6-trinitroaniline [24] (**20**) and 2-amino-3,5-dinitro-phenylamine (**21**) are known in the literature, but these intermediates were synthesized following different synthetic routes as described below. Quinoxalin-2(1*H*)ones **22**, **24** and chloroquinoxaline **3** are new compounds and were described below for the first time.

*4.1.2.1. 2,4,6-Trinitroaniline [24] (**20**).* A mixture of 2-chloro-1,3,5-trinitrobenzene [23] (**19**) (2 g, 8.1 mmol) and a saturated solution of NH_3 in 1-propanol (32 mL) was heated in a sealed tube at 100 °C for 3 h. On cooling, the reaction mixture was evaporated to dryness to give 1.1 g of **20**, as solid, in 75% yield; m.p. 189.5–191.5 °C [24] (methanol/H_2O).

*4.1.2.2. 2-Amino-3,5-dinitrophenylamine [25] (**21**).* Hydrogen sulfide was introduced into a mixture of 2,4,6-trinitroaniline [24] (**20**) (1 g, 4.37 mmol) and 30% aqueous solution NH_4OH (2.4 mL) in ethanol (100 mL) and heated under stirring at 45–50 °C for 30 min. Elemental sulfur was precipitated during the introduction of H_2S. The reaction mixture was cooled, and the solvent was evaporated to dryness to give 0.6 g of crude solid that was purified by flash chromatography over silica gel using petroleum ether and ethyl acetate as the eluent. 2-Amino-3,5-dinitrophenylamine [25] (**21**) was obtained in 90% yield; m.p. 215–218 °C [25] (ethanol).

^{1}H NMR ($CDCl_3$/DMSO-d_6): δ 8.40 (1H, d, $J = 2.4$ Hz), 8.64 (1H, d, $J = 2.4$ Hz), 7.76 (2H, s, exc. with D_2O), 7.61 (1H, d,), 5.51 (2H, s, exc. with D_2O).

*4.1.2.3. 5,7-Dinitro-3-phenylquinoxalin-2(1H)one (**22**) and 6,8-dinitro-3-phenylquinoxalin-2(1H)one (**24**).* To a mixture of

2-amino-3,5-dinitrophenylamine (**21**) (0.3 g, 1.51 mmol) and benzoyl formic acid (**23**) (0.36 g, 2.4 mmol) in ethanol (15 mL), 1.5 ml of 4 M HCl was added. The mixture was refluxed for 12 h. On cooling, the precipitate that formed was filtered and washed with ethanol. The crude solid was purified by silica gel column chromatography, eluting with a 8:2 mixture of petroleum ether and ethyl acetate to yield the isomer **24**. Further elution with a 1:1 mixture of petroleum ether and ethyl acetate gave the 5,7-dinitro-3-phenylquinoxalin-2(1*H*)one (**22**). Melting points, yields, analytical and spectroscopic data are reported below.

5,7-Dinitro-3-phenylquinoxalin-2(1*H*)one (**22**) was obtained at 75% yield; m.p. 317–319 °C (CH_3CN); TLC (petroleum ether/ethyl acetate 8:2): R_f 0.15; IR (nujol): ν 3240, 1680, 1620, 1530, 1350 cm^{-1}; UV (EtOH): λ_{max} 376, 297, 205 nm; ^1H NMR (DMSO-d_6): δ 13.21 (1H, br s, exc. with D_2O), 8.64 (1H, d, $J = 2.4$ Hz), 8.33 (2H, dd, $J = 6.4$ Hz and $J = 1.8$ Hz), 8.25 (1H, d, $J = 2.4$ Hz), 7.62–7.50 (3H, m); GC/MS: *m/z* 312 $[M]^+$. Anal. calcd. for $C_{14}H_8N_4O_5$: C, 53.85; H, 2.58; N, 17.94; found C, 53.65; H, 2.48; N, 17.84.

6,8-Dinitro-3-phenylquinoxalin-2(1*H*)one (**24**) was obtained at 2% yield; m.p. 257–258 °C (CH_3CN); TLC (petroleum ether/ethyl acetate 8:2): R_f 0.46; IR (nujol): ν 3240, 1690, 1615, 1530, 1340 cm^{-1}; UV (EtOH): λ_{max} 389, 282, 202 nm; ^1H NMR (DMSO-d_6): δ 13.38 (1H, s, exc. with D_2O), 8.98 (1H, d, $J = 3$ Hz), 8.92 (1H, d, $J = 3$ Hz), 8.35 (2H, dd, $J = 1.3$ Hz and $J = 7.2$ Hz), 7.65–7.50 (3H, m); GC/MS: *m/z* 312 $[M]^+$. Anal. calcd. for $C_{14}H_8N_4O_5$: C, 53.85; H, 2.58; N, 17.94; found C, 53.68; H, 2.49; N, 17.83.

*4.1.2.4. 5,7-Dinitro-3-phenyl-2-chloro-quinoxaline (**3**).* A suspension of **22** (1.46 g, 4.67 mmol) in $SOCl_2$ (26 mL) and 10 drops of DMF was heated under reflux until a clear solution was obtained (10 min), and for an additional 90 min. The $SOCl_2$ was removed under reduced pressure, and the residue was triturated with diethyl ether. A yellow solid of **3** (1.39 g) was filtered off (90% yield); m.p. 158.0–160 °C (C_2H_6O); TLC (petroleum ether/ethyl acetate 8:2): R_f 0.56; IR (nujol): ν 1620, 1530, 1325 cm^{-1}; UV (EtOH): λ_{max} 341, 241 nm; ^1H NMR ($CDCl_3$): δ 9.14 (1H, d, $J = 2.6$ Hz), 8.93 (1H, d, $J = 2.6$ Hz), 8.04 (2H, dd, $J = 8$ Hz and $J = 1.2$ Hz), 7.64–7.50 (3H, m); GC/MS: *m/z* 330 $[M]^+$. Anal. calcd. for $C_{14}H_7ClN_4O_4$: C, 50.85; H, 2.13; N, 16.94; found C, 50.75; H, 2.10; N, 16.73.

*4.1.2.5. General procedure for preparation of 5,7-dinitro-3-phenyl-2-anilino substituted quinoxalines (**11–17**).* A solution of **3** (150 mg, 0.45 mmol) in 1-propanol (15 mL) was obtained by heating under reflux. Then to the solution an excess (1.35 mmol) of the required substituted anilines (**4–10**) was added. Heating was maintained for different times as reported below. On cooling, the resulting precipitates were collected. In the case of the aminoester **10**, nucleophilic displacement of chlorine was carried out using ethanol to avoid the possible trans-esterification of the diethyl ester (**17**) as observed in other cases. The coloured precipitates formed were purified by flash chromatography over silica gel using petroleum ether and ethyl acetate as the eluent or by crystallization as reported below. Yields, reaction conditions, melting points, analytical and spectroscopical data are reported as follows.

*4.1.2.5.1. 2-[(4-Methoxy-phenyl)amino]-3-phenyl-5,7-dinitro-quinoxaline (**11**).* This compound was obtained at 84% yield starting from **3** (150 mg, 0.45 mmol) and 4-methoxy-phenylamine (**4**) (16 mg, 1.35 mmol) after 8 h; m.p. 249–250 °C (from CH_3CN); TLC (petroleum ether/ethyl acetate 8:2): R_f 0.31; IR (nujol): ν 3390, 1620, 1550, 1350 cm^{-1}; UV (EtOH): λ_{max} 309, 202 nm; ^1H NMR ($CDCl_3$/DMSO-d_6): δ 8.68 (1H, d, $J = 2.2$ Hz), 8.63 (1H, s, exc. with D_2O), 8.47 (1H, d, $J = 2.2$ Hz), 8.06–7.90 (2H, m), 7.70 (2H, d, $J = 9$ Hz), 7.66–7.55 (3H, m), 6.94 (2H, d, $J = 9$ Hz), 3.83 (3H, s); GC/MS: *m/z* 417 $[M]^+$. Anal. calcd. for $C_{21}H_{15}N_5O_5$: C, 60.43; H, 3.62; N, 16.78; found C, 60.23; H, 3.42; N, 16.58.

*4.1.2.5.2. 2-[(3,5-Dimethoxy-phenyl)amino]-3-phenyl-5,7-dinitro-quinoxaline (**12**).* This compound was obtained at 80% yield starting from **3** (150 mg, 0.45 mmol) and 3,5-dimethoxy-phenylamine (**5**) (210 mg, 1.35 mmol) after 10 h; m.p. 253–254 °C (from CH_3CN); TLC (petroleum ether/ethyl acetate 8:2): R_f 0.35; IR (nujol): ν 3390, 1605, 1550, 1345 cm^{-1}; UV (EtOH): λ_{max} 309, 205 nm; ^1H NMR ($CDCl_3$/DMSO-d_6): δ 8.90 (1H, s, exc. with D_2O), 8.71 (1H, d, $J = 2.2$ Hz), 8.56 (1H, d, $J = 2.2$ Hz), 7.97 (2H, dd, $J = 6$ Hz and $J = 2.2$ Hz), 7.70–7.60 (3H, m), 7.11 (2H, d, $J = 2.2$ Hz), 6.30–6.25 (1H, m), 3.81 (6H, s); GC/MS: *m/z* 447 $[M]^+$. Anal. calcd. for $C_{22}H_{17}N_5O_6$: C, 59.06; H, 3.83; N, 15.65; found C, 58.90; H, 3.63; N, 15.46.

*4.1.2.5.3. 2-[(3,4-Dimethoxy-phenyl)amino]-3-phenyl-5,7-dinitro-quinoxaline (**13**).* This compound was obtained at 90% yield starting from **3** (150 mg, 0.45 mmol) and 3,4-dimethoxy-phenylamine (**6**) (210 mg, 1.35 mmol) after 8 h; m.p. 213–215 °C (from C_2H_5O); TLC (petroleum ether/ethyl acetate 6:4): R_f 0.44; IR (nujol): ν 3390, 1605, 1535, 1350 cm^{-1}; UV (EtOH): λ_{max} 309, 205 nm; ^1H NMR ($CDCl_3$): δ 8.74 (1H, d, $J = 2.4$ Hz), 8.52 (1H, d, $J = 2.4$ Hz), 8.00–7.88 (2H, dd, $J = 6$ Hz and $J = 2.4$ Hz), 7.71–7.60 (3H, m), 7.48 (1H, s, exc. with D_2O), 7.39 (1H, d, $J = 2.4$ Hz), 7.20 (1H, dd, $J = 8.6$ Hz and $J = 2.4$ Hz), 6.91 (1H, d, $J = 8.6$ Hz), 3.95 (3H, s), 3.92 (3H, s); LC/MS: *m/z* 448 $[M + H]$, 470 $[M + Na]$, 486 $[M + K]$. Anal. calcd. for $C_{22}H_{17}N_5O_6$: C, 59.06; H, 3.83; N, 15.65; found C, 58.90, H, 3.50; N, 15.46.

*4.1.2.5.4. 2-[(3,4,5-Trimethoxy-phenyl)amino]-3-phenyl-5,7-dinitro-quinoxaline (**14**).* This compound was obtained at 95% yield starting from **3** (150 mg, 0.45 mmol) and 3,4,5-trimethoxy-phenylamine (**7**) (250 mg, 1.35 mmol) after 7 h; m.p. 228–229 °C (from CH_3CN); TLC (petroleum ether/ethyl acetate 6:4): R_f 0.38; IR (nujol): ν 3390, 1600, 1545, 1345 cm^{-1}; UV (EtOH): λ_{max} 312, 205 nm; ^1H NMR ($CDCl_3$): δ 8.72 (1H, d, $J = 2.4$ Hz), 8.53 (1H, d, $J = 2.4$ Hz), 7.98–7.86 (2H, m), 7.72–7.65 (3H, m), 7.50 (1H, s, exc. with D_2O), 7.02 (2H, s), 3.92 (3H, s), 3.87 (3H, s); GC/MS: *m/z* 477 $[M]^+$. Anal. calcd. for

$C_{23}H_{19}N_5O_7$: C, 57.86; H, 4.01; N, 14.67; found C, 58.16; H, 3.66; N, 14.59.

*4.1.2.5.5. 2-[(3,4-Dichloro-phenyl)amino]-3-phenyl-5,7-dinitro-quinoxaline (**15**).* This compound was obtained at 44% yield starting from **3** (150 mg, 0.45 mmol) and 3,4-dichlorophenylamine (**8**) (210 mg, 1.35 mmol) after 7 h; the compound was purified by silica gel column chromatography eluting with a 8:2 mixture of petroleum ether/ethyl acetate; m.p. 291–293 °C (from CH_3CN); TLC (petroleum ether/ethyl acetate 8:2): R_f 0.46; IR (nujol): ν 3390, 1605, 1535, 1350 cm^{-1}; UV (EtOH): λ_{max} 312, 205 nm; ^1H NMR ($CDCl_3$/DMSO-d_6): δ 9.51 (1H, br s, exc. with D_2O), 8.74 (1H, d, $J = 2.4$ Hz), 8.64 (1H, $J = 2.4$ Hz), 8.12 (1H, d, $J = 2.4$ Hz), 8.01–7.90 (3H, m), 7.68–7.60 (3H, m), 7.50 (1H, d, $J = 8.8$ Hz); GC/MS: *m/z* 456 $[M]^+$. Anal. calcd. for $C_{20}H_{11}Cl_2N_5O_4$: C, 52.65; H, 2.43; N, 15.35; found C, 52.43; H, 2.20; N, 15.22.

*4.1.2.5.6. 2-[(4-Fluoro-phenyl)amino]-3-phenyl-5,7-dinitro-quinoxaline (**16**).* This compound was obtained at 56% yield starting from **3** (150 mg, 0.45 mmol) and 4-fluoro-phenylamine (**9**) (150 mg, 1.35 mmol) after 1 h; the compound was purified by silica gel column chromatography eluting with a 8:2 mixture of petroleum ether/ethyl acetate; m.p. 259–263 °C (from CH_3CN); TLC (petroleum ether/ethyl acetate 8:2): R_f 0.34; IR (nujol): ν 3362, 1609, 1538, 1348 cm^{-1}; UV (EtOH): λ_{max} 312, 2063, 222, 205 nm; ^1H NMR ($CDCl_3$/DMSO-d_6): δ 9.27 (1H, br s, exc. with D_2O), 8.67 (1H, d, $J = 2.4$ Hz), 8.58 (1H, d, $J = 2.4$ Hz), 8.00–7.90 (2H, m), 7.89–7.80 (2H, m), 7.65–7.57 (3H, m), 7.12 (2H, t); GC/MS: *m/z* 405 $[M]^+$. Anal. calcd. for $C_{20}H_{12}FN_5O_4$: C, 59.26; H, 2.98; N, 17.28; found C, 59.02; H, 2.70; N, 17.00.

*4.1.2.5.7. N-[4(5,7-Dinitro-3-phenyl-quinoxalin-2-ylamino)-benzoyl]glutamic acid diethyl ester (**17**).* This compound was obtained at 61% yield using ethanol as solvent and starting from **3** (150 mg, 0.45 mmol) and *p*-amino-benzoyl-glutamic acid diethyl ester (**10**) (430 mg, 1.35 mmol) after 186 h; the compound was purified by silica gel column chromatography eluting with a 6:4 mixture of petroleum ether/ethyl acetate; m.p. 174–175 °C (from C_2H_6O); TLC (petroleum ether/ethyl acetate 6:4): R_f 0.32; IR (nujol): ν 3400, 3300, 1720, 1640, 1600, 1520, 1360 cm^{-1}; UV (EtOH): λ_{max} 428, 321, 204 nm; ^1H NMR ($CDCl_3$): δ 8.90 (1H, d, $J = 2.4$ Hz), 8.60 (1H, d, $J = 2.4$ Hz), 8.00–7.82 (4H, m and 1H exc. with D_2O), 7.82–7.65 (5H, m), 7.16 (1H, d, exch. with D_2O), 4.88–4.72 (1H, m), 4.26 (2H, q), 4.14 (2H, q), 2.62–2.09 (4H, m), 1.32 (3H, t), 1.25 (3H, t); GC/MS: *m/z* 616 $[M]^+$. Anal. calcd. for $C_{30}H_{28}N_6O_9$: C, 58.44; H, 4.58; N, 13.63; found C, 58.62; H, 4.20; N, 13.60.

*4.1.3. General procedure for preparation of 5,7-diamino-3-phenyl-2-anilino substituted quinoxalines (**2a–g**)*

A mixture of **11–17** (0.24–0.67 mmol) and an excess of hydrazine hydrate (2.9–10 mmol) in ethanol (15–127 mL), in the presence of 10% palladised charcoal was refluxed for the time reported below. The desired compounds were obtained by filtration of the ethanolic solution and evaporation in vacuo of the solvent. The crude solids were purified by recrystallization or by flash chromatography over silica gel as reported below.

*4.1.3.1. 2-[(4-Methoy-phenyl)amino]-3-phenyl-5,7-diaminoquinoxaline (**2a**).* This compound was obtained in 90% yield starting from **11** (150 mg, 0.36 mmol), hydrazine hydrate (150 mg, 3 mmol) and palladised charcoal (15 mg) in ethanol (81 mL) after 2 h and 45 min under reflux; m.p. 159–160 °C (from diethyl ether/petroleum ether); TLC (petroleum ether/ethyl acetate 4:6): R_f 0.34; IR (nujol): ν 3331, 3201, 1623, cm^{-1}; UV (EtOH): λ_{max} 396, 289, 228, 203 nm; ^1H NMR ($CDCl_3$): δ 7.75 (2H, dd, $J = 1.8$ Hz and $J = 7.8$ Hz), 7.61 (2H, d, $J = 9$ Hz), 7.60–7.49 (3H, m), 6.88 (2H, d, $J = 9$ Hz and 1H partially obscured, exc. with D_2O), 6.36 (1H, d, $J = 1.8$ Hz), 6.11 (1H, d, $J = 1.8$ Hz), 4.30 (2H, br s, exc. with D_2O), 3.80 (3H, s); GC/MS: *m/z* 357 $[M]^+$. Anal. calcd. for $C_{21}H_{19}N_5O$: C, 70.57; H, 5.36; N, 19.59; found C, 70.21; H, 5.20; N, 15.40.

*4.1.3.2. 2-[(3,5-Dimethoxy-phenyl)amino]-3-phenyl-5,7-diamino-quinoxaline (**2b**).* This compound was obtained at 71% yield starting from **12** (250 mg, 0.56 mmol), hydrazine hydrate (260 mg, 5.2 mmol) and palladised charcoal (25 mg) in ethanol (125 mL) after 1 h under reflux; m.p. 148–150 °C (from $CH_4O + H_2O$); TLC (petroleum ether/ethyl acetate 4:6): R_f 0.49; IR (nujol): ν 3420, 3360, 1600, 1200, 1070 cm^{-1}; UV (EtOH): λ_{max} 293, 223, 204 nm; ^1H NMR (DMSO-d_6): δ 8.08 (1H, s, exc. with D_2O), 7.88–7.78 (2H, dd, $J = 6.6$ Hz and $J = 1.2$ Hz), 7.62–7.42 (3H, m), 7.12 (2H, d, $J = 2$ Hz), 6.12 (1H, t), 6.10 (1H, d, $J = 2$ Hz), 6.03 (1H, d, $J = 2$ Hz), 5.64 (2H, br s, exc. with D_2O), 5.57 (2H, br s, exc. with D_2O), 3.73 (6H, s); GC/MS: *m/z* 387 $[M]^+$. Anal. calcd. for $C_{22}H_{21}N_5O_2$: C, 68.20; H, 5.46; N, 18.08; found C, 68.18; H, 4.26; N, 18.00.

*4.1.3.3. 2-[(3,4-Dimethoxy-phenyl)amino]-3-phenyl-5,7-diamino-quinoxaline (**2c**).* This compound was obtained at 90% yield starting from **13** (300 mg, 0.67 mmol), hydrazine hydrate (495 mg, 10 mmol) and palladised charcoal (230 mg) in ethanol (24 mL) after 30 min under reflux; the compound was purified by silica gel column chromatography eluting with a 4:6 mixture of petroleum ether/ethyl acetate; m.p. 181–182 °C (from $CH_4O + H_2O$); TLC (petroleum ether/ethyl acetate 4:6): *Rf* 0.61; IR (nujol): ν 3420, 3370, 1625, 1200, 1070 cm^{-1}; UV (EtOH): λ_{max} 400, 290, 225, 202 nm; ^1H NMR (DMSO-d_6): δ 7.90 (1H, s, exc. with D_2O), 7.79 (H, dd, $J = 6.4$ Hz and $J = 1.4$ Hz), 7.55 (1H, d, $J = 2.2$ Hz), 7.53–7.44 (3H, m), 7.26 (1H, dd, $J = 6.6$ Hz and $J = 2.2$ Hz), 6.87 (1H, d, $J = 8.8$ Hz), 6.03 (1H, d, $J = 2.2$ Hz), 5.96 (1H, d, $J = 2.2$ Hz), 5.58 (1H, br s, exc. with D_2O), 5.49 (2H, br s, exc. with D_2O), 3.74 (3H, s), 3.72 (3H, s); LC/MS: *m/z* 388 $[M + H]$. Anal. calcd. for $C_{22}H_{21}N_5O_2$: C, 68.20; H, 5.46; N, 18.08; found C, 67.24; H, 5.10; N, 18.07.

*4.1.3.4. 2-[(3,4,5-Trimethoxy-phenyl)amino]-3-phenyl-5,7-diamino-quinoxaline (**2d**).* This compound was obtained at 46% yield starting from **14** (150 mg, 0.31 mmol), hydrazine hydrate

(145 mg, 2.9 mmol) and palladised charcoal (15 mg) in ethanol (60 mL) after 1 h under reflux; m.p. 175–177 °C (from $CH_4O + H_2O$); TLC (petroleum ether/ethyl acetate 4:6): R_f 0.41; IR (nujol): ν 3425, 3350, 1600, 1200, 1070 cm^{-1}; UV (EtOH): λ_{max} 398, 292, 202 nm; ^1H NMR (DMSO-d_6): δ 8.01 (1H, s, exc. with D_2O), 7.79 (H, dd, $J = 6.4$ Hz and $J = 1.4$ Hz), 7.60–7.40 (3H, m), 7.27 (2H, s), 6.05 (1H, d, $J = 2.2$ Hz), 5.99 (1H, d, $J = 2.2$ Hz) 5.60 (2H, br s, exc. with D_2O), 5.53 (2H, br s, exc. with D_2O), 3.75 (6H, s), 3.62 (3H, s); GC/MS: *m/z* 417 $[M]^+$. Anal. calcd. for $C_{23}H_{23}N_5O_3$: C, 66.17; H, 5.55; N, 16.78; found C, 66.00; H, 5.32; N, 16.57.

*4.1.3.5. 2-[(3,4-Dichloro-phenyl)amino]-3-phenyl-5,7-diamino-quinoxaline (**2e**).* This compound was obtained at 54% yield starting from **15** (200 mg, 0.44 mmol), hydrazine hydrate (320 mg, 6.4 mmol) and palladised charcoal (20 mg) in ethanol (15 mL) after 10 min under reflux; the compound was purified by silica gel column chromatography eluting with a 6:4 mixture of petroleum ether/ethyl acetate; m.p. 192–193 °C (from CH_4O); TLC (petroleum ether/ethyl acetate 6:4): R_f 0.4; IR (nujol): ν 3435, 3333, 1633 cm^{-1}; UV (EtOH): λ_{max} 301, 221, 203 nm; ^1H NMR ($CDCl_3$/DMSO-d_6): δ 8.22 (1H, d, $J = 2.4$ Hz), 7.76 (2H, dd, $J = 1.8$ Hz and $J = 7.4$ Hz), 7.62–7.50 (3H, m), 7.47 (1H, d, $J = 2.4$ Hz), 7.35 (1H, t), 6.38 (1H, d, $J = 2.2$ Hz), 6.20 (1H,d, $J = 2.2$ Hz), 5.11 (2H, br s, exc. with D_2O), 4.66 (2H, br s, exc. with D_2O); LC/MS: *m/z* 396 $[M + H]$. Anal. calcd. for $C_{20}H_{15}Cl_2N_5$: C, 60.62; H, 3.82; N, 17.67; found C, 60.42; H, 3.53; N, 17.57.

*4.1.3.6. 2-[(4-Fluoro-phenyl)amino]-3-phenyl-5,7-diamino-quinoxaline (**2f**).* This compound was obtained at 77% yield starting from **16** (150 mg, 0.37 mmol), hydrazine hydrate (250 mg, 5 mmol) and palladised charcoal (15 mg) in ethanol (18 mL) after 10 min under reflux; m.p. 158–161 °C (from $CH_4O + H_2O$); TLC (petroleum ether/ethyl acetate 1:1): R_f 0.42; IR (nujol): ν 3430, 3310, 1630 cm^{-1}; UV (EtOH): λ_{max} 392, 291, 225, 202 nm; ^1H NMR ($CDCl_3$/DMSO-d_6): δ 7.80–7.65 (7H, m), 7.60 (2H, d, $J = 6.2$ Hz), 7.02 (2H, t), 6.35 (1H, d, $J = 2.6$ Hz), 6.14 (2H, d, $J = 2.6$ Hz), 4.72 (2H, br s, exc. with D_2O), 4.20 (2H, br s, exc. with D_2O); GC/MS: *m/z* 345 $[M]^+$. Anal. calcd. for $C_{20}H_{16}FN_5$: C, 69.55; H, 4.67; N, 20.28; found C, 69.44; H, 4.57; N, 20.12.

*4.1.3.7. N-[4-[(5,7-Diamino-3-phenyl-quinoxalin-2-yl)amino]-benzoyl]glutamic acid diethyl ester (**2g**).* This compound was obtained at 76% yield starting from **17** (150 mg, 0.24 mmol), hydrazine hydrate (170 mg, 3.5 mmol) and palladised charcoal (15 mg) in ethanol (18 mL) after 30 min under reflux; the compound was purified by silica gel column chromatography eluting with a 4:6 mixture of petroleum ether/ethyl acetate; m.p. 164–165 °C (from CH_4O); TLC (petroleum ether/ethyl acetate 4:6): R_f 0.24; IR (nujol): ν 3430, 3310, 1730, 1640, 1600 cm^{-1}; UV (EtOH): λ_{max} 379, 295, 208 nm; ^1H NMR ($CDCl_3$): δ 7.81 (4H, s), 7.73 (2H, d, $J = 7$ Hz), 7.62–7.50 (3H, m), 7.18 (1H, s, exc. with D_2O), 6.99 (1H, d, exc. with D_2O), 6.43 (1H, d, $J = 1.6$ Hz), 6.17 (2H, d, $J = 1.6$ Hz), 4.24 (2H, q), 4.11 (2H, q), 4.00 (2H, br s, exc. with D_2O), 2.60–2.03 (4H, m), 1.31 (3H, t), 1.22 (3H, t); LC/MS: *m/z* 557 $[M + H]$. Anal. calcd. for $C_{30}H_{32}N_6O_5$: C, 64.73; H, 5.79; N, 15.10; found C, 64.67; H, 5.62; N, 15.01.

4.2. Pharmacology

Compounds **2a–g** were evaluated for in vitro activity against sixty human tumor cell lines, derived from nine cancer types (leukemia, non-small cell lung, colon, CNS, melanoma, ovarian, renal, prostate, and breast cancers). For each compound, dose–response curves against each cell line were measured at a minimum of five concentrations at 10-fold dilutions. A protocol of 48 h continuous drug exposure was used, and a sulforhodamine B (SRB) protein assay has been used to estimate cell viability or growth [35].

4.3. Enzymology assays

All the reagents used for enzyme purification and enzyme kinetics were of purity grade. 6-*R*-N^5,N^{10}-Methylentetrahydrofolate is a generous gift of Eprova (Schaffhausen, Switzerland). The hDHFR, hTS, EcTS, LcTS plasmids and strains were supplied by Dr. D.V. Santi (University of California, San Francisco, USA; present address Kosan, San Francisco), and Dr. G.F. Maley (New York State Department of Health, New York). The enzymatic assays have been run on spectrophotometer UV–vis, Beckman DU 640, equipped with a thermostat circulating bath HAAKE F3C.

The expression and purification of LcTS, EcTS, hTS and hDHFR was done following known procedures as already reported [36–40]. The enzyme preparations were >95% homogeneous as visualized by SDS (sodium dodecyl sulfate)-polyacrylamide gel electrophoresis. The purified enzymes were stored at −80 °C in 10 mM phosphate buffer, pH 7.0, and 0.1 mM EDTA.

The TS activity was determined spectrophotometrically by steady-state kinetic analysis, following the increasing absorbance at 340 nm due to the oxidation reaction of N^5,N^{10}-methylenetetrahydrofolate (mTHF) to dihydrofolate (DHF) [41]. One milliliter of reaction solution was formed by standard assay buffer pH 7.4, dUMP (100 μM), 6(R,S)-1-CH_2CH_4-folate (140 μM) (SIGMA), enzyme (0.07 μM). Assays were performed at 20 °C in the standard assay buffer formed by TES (*N*-tris(hydroxymethyl)methyl-2-aminoethanesulfonic acid) (50 mM) at pH 7.4, $MgCl_2$ (25 mM), formaldehyde (6.5 mM), EDTA (1 mM), and 2-mercaptoethanol (75 mM).

DHFR catalyzes the NADPH-dependent reduction of dihydrofolate (DHF) to tetrahydrofolate (THF). The assays were run spectrophotometrically by measuring the decrease in absorbance at 340 nm upon DHF reduction at 25 °C. One enzyme unit is defined as 1 nmol of DHF reduced per minute. The reaction mixture was formed by 50 μM TES, pH 7.0, EDTA 1 μM, 1-mercaptoethanol 75 μM, NADPH 100 μM, DHF 58.03 μM [42].

Stock solutions of the inhibitors were prepared in DMSO (dimethyl sulfoxide) and stored at −20 °C until use. The inhibition pattern for all compounds was determined by steady-state kinetic analysis of the dependence of enzyme activity on folate concentration at varying inhibitor concentrations. All compounds showed competitive inhibition. Ki values were obtained from the linear least-squares fit of the residual activity as a function of inhibitor concentration, using suitable equations for competitive inhibition [43]. Each experiment was repeated at least three times, and no individual measurement differed by more than 20% from the mean. The effect of increasing DMSO concentration in the TS assay mixture was studied, and it was observed that no change in TS activity was seen at concentrations up to 8% DMSO (personal communication).

4.4. Molecular docking

The program AutoDock 3.0.5 was used for docking [44]. The protein structure of hDHFR was taken from the crystal structure of the ternary complex with NADPH and MTX (1U72), available in the PDB [18–20,22]. Polar hydrogen atoms were added to the protein with the WHATIF program [45]. Solvation parameters and atomic partial charges were assigned to the protein using the programs q.kollua and addsol, included in the AutoDock program suite. Polar hydrogen atoms were added and atomic charges were assigned to the cofactor using the AutoDockTools program [46]. The ligand (**2a–d**) structures were built with the ChemOffice suite of programs [47]. Atomic partial charges were assigned using the AutoDockTools program. A grid with sides of 20.25, 24 and 20.25 Å long, centered on the active site of the enzyme was defined. This grid is large enough to cover the active site of the enzyme. A Lamarckian genetic algorithm was used to generate 100 bound conformations for each ligand. All single bonds of the ligands were allowed to rotate during the calculation. The ga_pop_size parameter was set at 200. All other settings were kept as default. On the basis of the clustering histogram output from the AutoDock program, the lowest energy conformation of the most populated low energy cluster was selected.

Acknowledgments

The authors are grateful to the staff of the Department of Health and Human Services, National Cancer Institute, Bethesda, MD, USA, for the anti-cancer screening. This work was supported by MIUR (Italian Ministry of University and Research) Cofin04_2004030405_004 CSTMPL and Cofin04 Paglietti.

References

[1] I.M. Kompis, K. Isalam, R.L. Then, Chem. Rev. 105 (2005) 593 and references cited therein.
[2] N. Nemati, U.S. Pat. Appl. Pubbl. US 2006 235 034. Chem. Abstr. 145 (2005) 920.
[3] M. Loriga, M. Fiore, P. Sanna, G. Paglietti, Farmaco 50 (1995) 289.
[4] M. Loriga, M. Fiore, P. Sanna, G. Paglietti, Farmaco 51 (1996) 559.
[5] M. Loriga, S. Piras, P. Sanna, G. Paglietti, Farmaco 52 (3) (1997) 157.
[6] M. Loriga, P. Moro, P. Sanna, G. Paglietti, Farmaco 52 (8–9) (1997) 531.
[7] G. Vitale, P. Corona, M. Loriga, G. Paglietti, Farmaco 53 (1998) 139.
[8] G. Vitale, P. Corona, M. Loriga, G. Paglietti, Farmaco 53 (1998) 150.
[9] P. Corona, G. Vitale, M. Loriga, G. Paglietti, M.P. Costi, Farmaco 53 (1998) 480.
[10] G. Vitale, P. Corona, M. Loriga, G. Paglietti, Farmaco 53 (1998) 594.
[11] P. Corona, G. Vitale, M. Loriga, G. Paglietti, Farmaco 55 (2000) 77.
[12] S. Piras, M. Loriga, G. Paglietti, Farmaco 57 (2002) 1.
[13] M. Loriga, S. Piras, G. Paglietti, M.P. Costi, A. Venturelli, Farmaco 58 (2003) 51.
[14] S. Alleca, P. Corona, M. Loriga, G. Paglietti, R. Loddo, V. Mascia, B. Busonera, P. La Colla, Farmaco 58 (2003) 639.
[15] S. Piras, M. Loriga, G. Paglietti, Farmaco 59 (2004) 189.
[16] P. Corona, G. Vitale, M. Loriga, G. Paglietti, P. La Colla, G. Collu, G. Sanna, R. Loddo, Eur. J. Med. Chem. 41 (2006) 1102–1107.
[17] S. Piras, M. Loriga, A. Carta, G. Paglietti, M.P. Costi, S. Ferrari, J. Heterocycl. Chem. 43 (2006) 541.
[18] H.M. Berman, J. Westbrook, Z. Feng, G. Gilliland, T.N. Bhat, H. Weissig, I.N. Shindyalov, P.E. Bourne, Nucleic Acids Res. 28 (2000) 235.
[19] H.M. Berman, K. Henrick, H. Nakamura, Nat. Struct. Biol. 10 (12) (2003) 980.
[20] http://www.pdb.org/
[21] W.S. Lewis, V. Cody, N. Galitsky, J.R. Luft, W. Pangborn, S.K. Chunduru, H.T. Spencer, J.R. Appleman, R.L. Blakley, J. Biol. Chem. 270 (1995) 5057.
[22] V. Cody, J.R. Luft, W. Pangborn, Acta Crystallogr. D. Biol. Crystallogr. 61 (2005) 147.
[23] E.T. Borrows, J.C. Clayton, B.A. Hems, A.G. Long, J. Chem. Soc. (1949) 190.
[24] R.J.W. Le Fèvre, D.D. Moir, E.E. Turner, J. Chem. Soc. (1927) 2330.
[25] R. Nietzki, H. Hagenback, Chem. Ber. 30 (1897) 543.
[26] M. Loriga, A. Nuvole, G. Paglietti, J. Chem. Res., Synop. (1989) 202; J. Chem. Res., Miniprint (1989) 1553.
[27] G.O. Dudek, Spectrochim. Acta 19 (1963) 691.
[28] C. MacLean, E.L. Mackor, Mol. Phys. 3 (1960) 223.
[29] R.H. Martin, N. Defay, F. Greets-Evrard, Tetrahedron 20 (1964) 1505.
[30] S.N. Bannore, J.L. Bose, A.A. Thakar, M.S. Wadia, Indian J. Chem. 13 (1975) 609.
[31] M.R. Boyd, Am. Assoc. Cancer Res. 30 (1989) 652.
[32] A. Monks, D. Scudiero, P. Skehan, R. Shoemaker, K. Poull, D. Vistica, C. Hose, J. Langley, P. Cronise, A. Vaigro-Wolff, M. Gray-Goodrich, H. Cambell, M. Boyd, J. Natl. Cancer Inst. 83 (1991) 757.
[33] J.N. Weinstein, T.G. Myers, P.M. O'Connor, S.H. Friend, A.J. Fornance Jr., K.W. Kohn, T. Fojo, S.E. Bates, L.V. Rubinstein, N.L. Anderson, J.K. Buolamwini, W.W. van Osdol, A.P. Monks, D.A. Scudiero, E.A. Sausiville, D.W. Zaharevitz, B. Bunow, V.N. Viswanadhan, G.S. Johnson, R.E. Wittes, K.D. Paull, Science 275 (1997) 343.
[34] <http://dtp.nci.nih.gov/>.
[35] P. Skehan, R. Storeng, D. Scudiero, A. Monks, J. Mc Mahon, D. Vistica, J.T. Warren, H. Bokesh, S. Kenney, M.R. Boyd, J. Natl. Cancer Inst. 82 (1990) 1107.
[36] J.T. Kealey, D.V. Santi, Prot. Expr. Purif. 4 (1992) 380.
[37] G.F. Maley, F. Maley, J. Biol. Chem. 263 (1988) 7620.
[38] V. Davisson, W. Sirawaraporn, D.V. Santi, J. Biol. Chem. 264 (1989) 9145.
[39] J.G. Dann, G. Ostler, R.A. Bjur, W.R. King, P. Scudder, G.C.K. Roberts, S.V. Burgen, Biochem. J. 157 (1976) 559.
[40] M.P. Costi, A. Gelain, D. Barlocco, S. Ghelli, F. Soragni, F. Reniero, T. Rossi, A. Ruberto, C. Guillou, A. Cavazzuti, C. Casolari, S. Ferrari, J. Med. Chem. 49 (20) (2006) 5958.
[41] A.L. Pogolotti Jr., P.V. Danenberg, D.V. Santi, J. Med. Chem. 29 (1986) 478.
[42] T.D. Meek, E.P. Garvey, D.V. Santi, Biochemistry 24 (1985) 678.

[43] I.H. Segel, Enzyme Kinetics: Behaviour and Analysis of Rapid Equilibrium and Steady-state Enzyme Systems, John Wiley and Sons, Inc., New York, 1975, 105.
[44] G.M. Morris, D.S. Goodsell, R.S. Halliday, R. Huey, W.E. Hart, R.K. Belew, A.J. Olson, J. Comput. Chem. 19 (1998) 1639.
[45] G. Vriend, J. Mol. Graph. 8 (1990) 52.
[46] Molecular Graphics Laboratory, The Scripps Research Institute.
[47] Cambridge Soft Corporation.
[48] J.I. DeGraw, P.H. Christie, H. Tagawa, R.L. Kisliuk, Y. Gaumont, F.A. Schmid, F.M. Sirotnak, J. Med. Chem. 29 (1986) 1056.